River Flow 2010 - Dittrich, Koll, Aberle & Geisenhainer (eds) - © 2010 Bundesanstalt für Wasserbau ISBN 978-3-939230-00-7

3D turbulent flow field at square pier in a gravel scour hole

R. Diab & U. Zanke
Institute for Hydraulic and Water Resources Engineering, Technische Universität Darmstadt, Germany
O. Link
Department of Civil Engineering, University of Concepción, Chile

ABSTRACT: Bridge elements in a flow induce turbulence and vorticity that increase the risk of sediment bed scouring. The turbulent flow field around a square cylinder in a plane and equilibrium scoured bed was investigated experimentally. The cylinder was embedded in a uniform gravel bed with d50 = 3.25 mm. Experiments were conducted in a relative large laboratory flume with 37 m length, 2 m width and 1 m depth at the laboratory of the Institute for Hydraulic and Water Resources Engineering of the Darmstadt University of Technology, Germany. Experiments were conducted under the clear-water condition. Point flow velocities and turbulent intensities were measured with the acoustic doppler velocimeter (ADV). Measurements were carried out at the pier front, sides and wake in azimuthal planes with θ = 0, 45, 90, 135, and 180º. Results show the time-averaged velocity field, turbulent intensities and turbulent kinetic energy at different distances from the original bed level. These results are useful for calibration and validation of three dimensional flow models and turbulence closure models as well.

Keywords: Pier, Scour, Gravel, Turbulent flow field, ADV

1 INTRODUCTION

Turbulence and induced secondary flow field in the form of vortices around the bridge elements are considered to be the main cause of local scour. So, it has been investigated intensively in the last years both experimentally and numerically (e.g. Zanke 1982, Muzzammil and Gangadhariah 2003, Unger and Hager 2007, Dey and Raikar 2007, Kirkil et al. 2008, Link et al. 2008a, Gobert et al. 2009, Kirkil et al. 2009). While most of these articles focused on scouring around circular pier in sand beds, only very few studies on scouring around non-circular piers in gravel bed are available in the literature. Raikar and Dey (2005a, b) presented experimental results on scour in uniform gravels, analyzing the effect of gravel size and gradation on equilibrium scour depth. In both mentioned studies, it was concluded that significant differences in scour are expected depending on the sediment type i.e. sand or gravel. Diab et al. (2009) presented experimental measurements of the distribution of time-averaged velocity components and flow vectors around a square pier in gravel.

In this article, experimental investigation of 3D turbulent flow field around a square cylinder in a plane bed and an equilibrium gravel scour-hole is presented.

2 EXPERIMENTATIONS

Experiments were carried out in a large laboratory flume with 37m length, 2 m wide and 1 m deep. The flume has glass side-walls 26m long that help to observe and monitor the flow and sediment transport. A plexiglas square pier 0.20x0.20m, side facing the approaching flow, was mounted in the middle of a working section located 16 m downstream of the flume entrance and having a length of 4 m, width of 2 m and depth of 0.55 m. A false bottom made of concrete plates was installed to avoid the filling of the whole flume with sediment. The plates rested on bricks, 0.5 m above the original flume bottom. The sides of the working section were coated with absorbing material to avoid secondary flow.

The employed bed material was gravel with grain sizes ranging between 2.25 and 4.00 mm and a sediment size for which 50% of the sediment is finer, d_{50} of 3.25 mm. The natural repose angle of sediment particles ϕ was 35.5°. The geometric standard deviation of the particle sizes was $\sigma_g = [d_{84.1}/d_{15.9}]^{0.50}$ =1.20 and therefore the sediment was considered to be uniform (Dey et al. 1995). The critical shear stress for the initiation of motion of isolated sediment particles was τ_{cr} = 0.65 KN/m_2. Experiments were conducted over 100 hours with section-averaged flow depth of h = 0.30 m and velocity U_m = 0.616 m/s which was 95% of the critical velocity for initiation of sediment motion at an undisturbed plane bed. An acoustic Doppler velocimeter (ADV), developed by SonTek (5 cm down-looking and sampling rate 50 Hz), was used to measure the instantaneous 3D velocity. In order to obtain statistically time independent average-velocity components, the sampling durations were 3-4 min. Two experiments were conducted, namely (1) with a plane sediment bed and (2) in an equilibrium scour hole. Figure 1 shows the coordinate system for the velocity measurements.

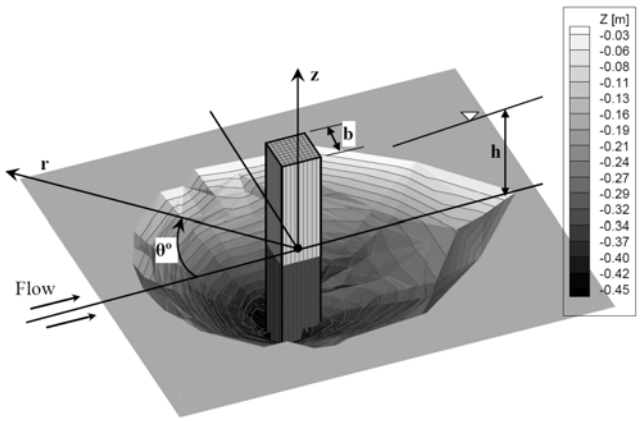

Figure 1. Measuring Coordinate System and scour pattern after t =100 hours.

Bed topography was measured using a laser distance sensor (LDS) with an accuracy of ±0.30 mm which was located inside the plexiglas pier. The sensor was driven by step-motors, for record of various vertical profiles in different half azimuthal planes. Flow depth was adjusted by a tail gate at the end of the flume, and measured with ultrasonic distance sensors (UDS) placed along the flume. For details on measuring system and scour measurements please refer to Link et *al.* (2008b) and Diab et *al.* (2008). Figure 2 shows the experimental set-up.

Figure 2. Experimental set-up with plane (upper) and scoured bed (lower).

The ADV measurements were carried out at pier front, sides and wake in azimuthal planes with θ = 0, 45, 90, 135 and 180º at different distances from the original gravel bed level with z = 1, 3, 5, 7, 11, 13, 15, 17, 19, 23 cm. The reference level z = 0 correspond to the original flat bed elevation. The lowest point of ADV Reading was 1 cm above the bed.

3 RESULTS AND ANALYSIS

The presented experiment was conducted over 100 hours till scouring approached equilibrium. Scouring started and progressed fast at the pier sides, the deepest point being found at θ = 45º during the first 3000s of experimentation. Later, maximum depth inside the scour-hole was observed at the pier front with θ = 0º. At the pier wake with θ = 180º, deposition region was observed during the first 3240s then scour surrounded the pier perimeter. Final maximum scour depth in the equilibrium scour hole was 45.80 cm that was equal to 2.29 times the width of the pier width. Scour-hole side slopes diminished with θ, changing from an average of 36 to 16º at planes with θ = 0 and 180º. For more details on the geometric properties of developing and equilibrium scour holes please refer to Diab et al. (2010).

3.1 *Velocity Measurements*

Figure 3 shows the contours of the time-average absolute velocity, $U_{total} = \sqrt{u^2 + v^2 + w^2}$ at azimuthal-half planes with θ = 0, 45, 90, 135 and 180º in cm/s for plane bed (left) and equilibrium scour hole (right). U_{total} is a scalar quantity

that represents the intensity of the total velocity. For the plane bed, the magnitude of U_{total} increases with increasing θ from 0 to 135º then diminishes towards the pier wake with θ = 180º. At θ = 45º, the existence of flow separation due to the pier edge cause smaller values of U_{total}. A region of rapid changing in U_{total} near the bed is clear from the concentration of contour lines. In the equilibrium scour hole, U_{total} values are smaller than those over the plane bed. At θ = 0º, the vertical flow component and the absence of the tangential velocity u is evident. At θ = 90º, the tangential velocity u is a predominant flow feature. While the vertical flow and the tangential velocity characterize together the flow at θ = 135º. At the pier wake with θ = 180º, the lower values of U_{total} near the pier face is observed due to the back flow and the lower values of the radial velocity and it grows toward the downstream.

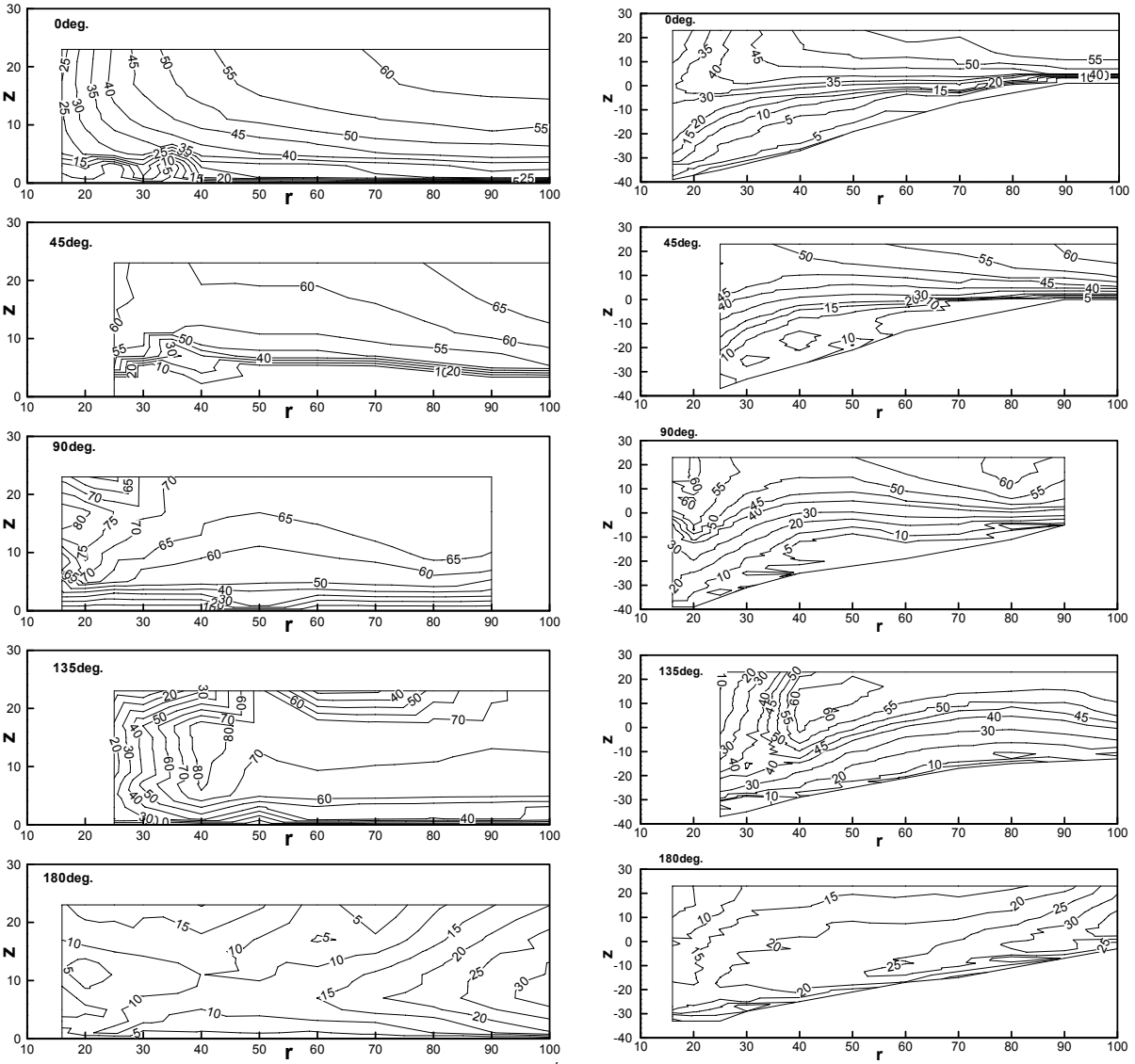

Figure 3. Contours of time-averaged absolute velocity $\sqrt{u^2 + v^2 + w^2}$ (in cm/s) at azimuthal planes with θ =0, 45, 90, 135 and 180º for plane bed (left) and for scoured bed (right).

Figure 4 shows the contours of the time-average vertical velocity vector, $\sqrt{v^2 + w^2}$ at azimuthal planes with θ = 0, 45, 90, 135 and 180º in cm/s for plane bed (left) and equilibrium scour hole (right). The characteristics of the horseshoe vortex and the strong downflow inside the scour hole at the pier front and sides with θ = 0 to 60º are observed. The flow is horizontal above the scour hole for r >2b for the solid bed and r > 3b for the equilibrium phase between θ = 0 to 45º. Then the flow gradually curves down towards the pier. At θ = 90 and 135º, the flow becomes outwards the pier above the scour hole with low circulation motion. At θ = 180º, it shows a swirl motion near the pier with r < 2b, and then the flow becomes gradually outwards the pier over the flow depth in the solid bed case. For the solid bed, the horseshoe vortex is not distinct while it becomes strong at the pier front for the equilibrium phase and decreases with increase in θ.

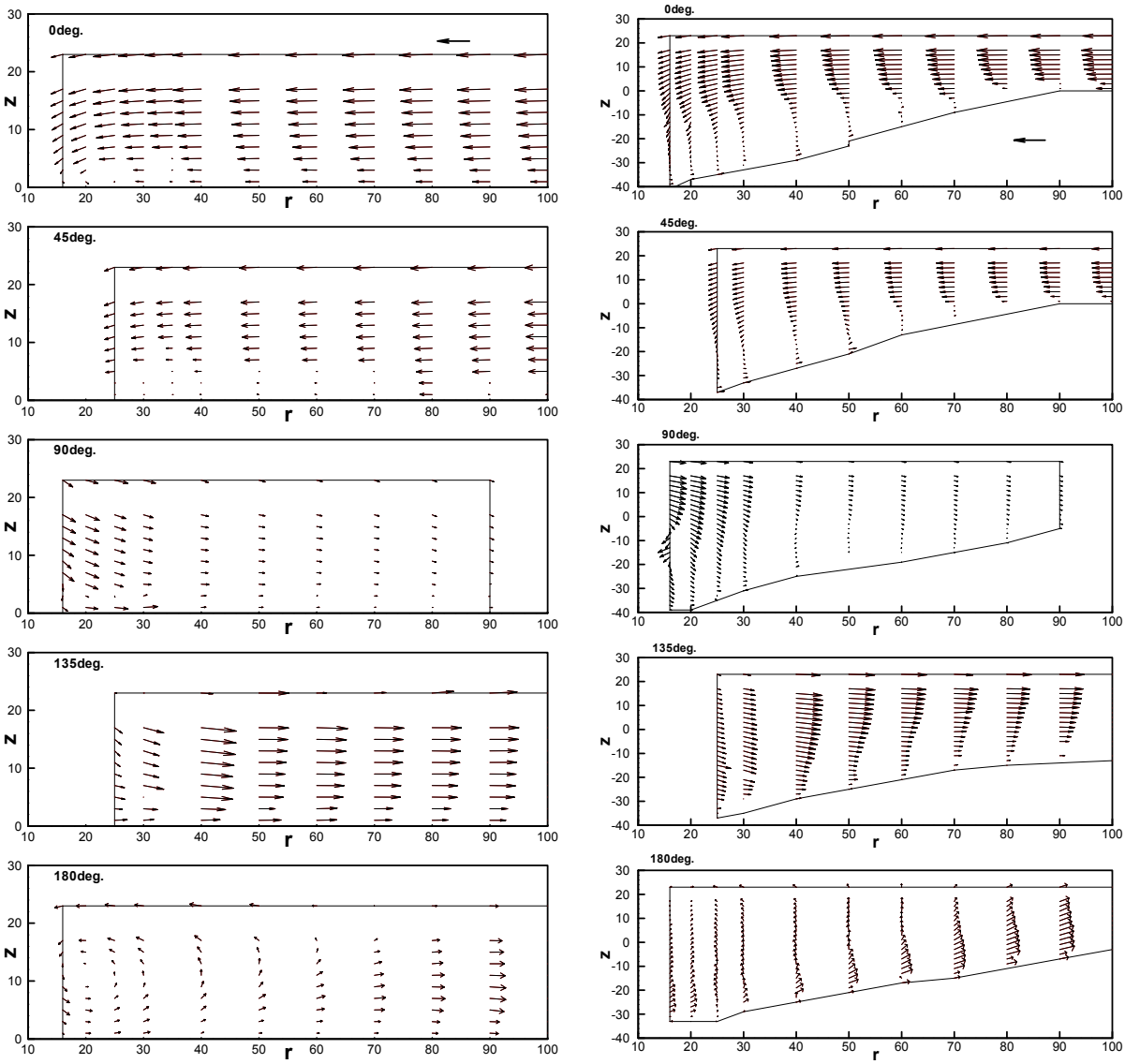

Figure 4. Velocity vector $\sqrt{v^2 + w^2}$ (in cm/s) at azimuthal planes with θ =0, 45, 90, 135 and 180º for plane bed (left) and for scoured bed (right).

3.2 *Turbulence Field*

The pattern of turbulence intensities $\sqrt{u'u'}$, $\sqrt{v'v'}$, and $\sqrt{w'w'}$ (in cm/s) at azimuthal half-planes with θ =0, 90 and 180º for plane bed (left) and for scoured bed (right) are shown in figures 5, 6 an 7. The distribution of the turbulent intensities at different azimuthal planes is identical. The radial and tangential components of turbulent intensities are larger than the vertical one. At the pier front and sides, with θ = 0 and 90º, the magnitudes $\sqrt{u'u'}$, $\sqrt{v'v'}$ and $\sqrt{w'w'}$ decrease with the vertical distance from the bed. At θ = 180º on the scoured bed, the turbulent intensities first increase with z until an imaginary line of separation at a depth of 0.45-0.75 times the local scour depth inside the scour hole (see Diab et al. 2009), then decrease again vertically, forming a core of high turbulent intensity over whole of the scour hole. At planes with θ = 0 and 90º, the turbulence intensities increase with decreasing distance to the pier when r < 2b due to the down flow and flow separation. The maximum turbulent intensity was found as a core at the upstream pier face.

The contours of the turbulent kinetic energy TKE $[=0.50(\overline{u'u'} + \overline{v'v'} + \overline{w'w'})]$ at the pier front, sides and wake with θ = 0, 90 and 180º for plane and scored beds are plotted in figure 8. The distribution of *TKE* is similar to that of the turbulent intensity components. *TKE* values increase with θ and with decreasing *r* and *z*. The effect of turbulence leads to much more scouring in front of the pier than at the pier wake where up flow occurs.

Unfortunately- to the best of our knowledge- very few researches on scouring and flow field around square pier in gravel beds are available for comparison of the presented results. Nevertheless the results of Dey and Raikar (2007) show a similar trend.

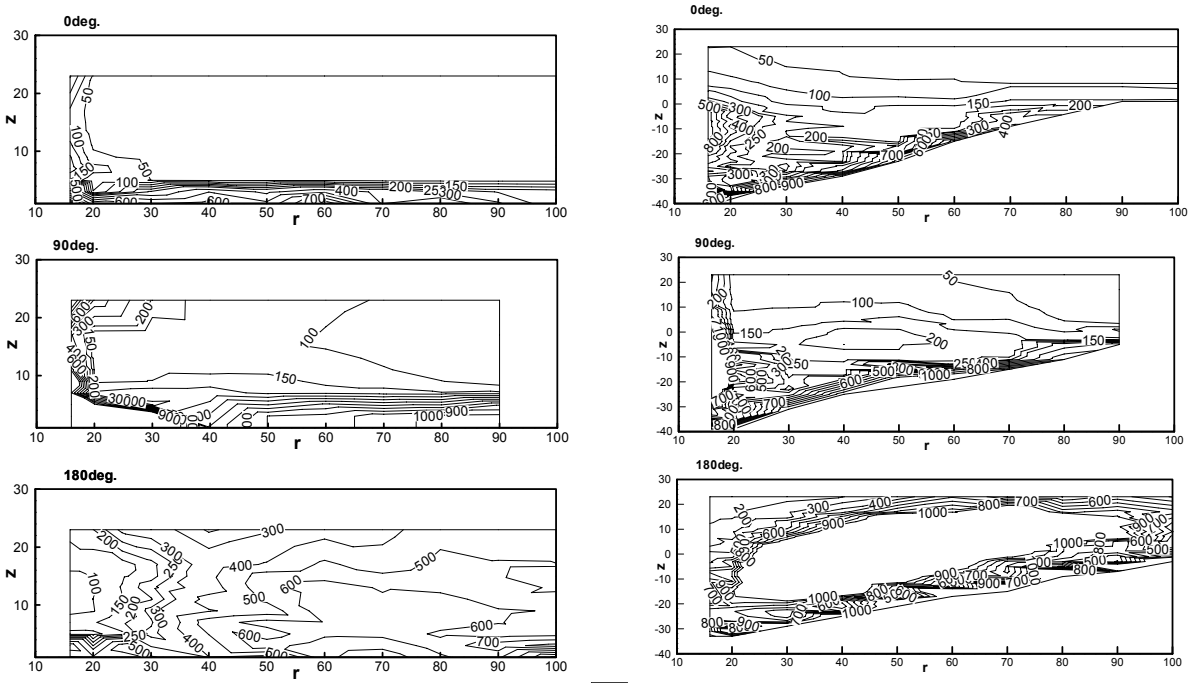

Figure 5. Contours of tangential turbulence intensity $\sqrt{u'u'}$ (in cm/s) at azimuthal planes with θ =0, 90 and 180º for plane bed (left) and for scoured bed (right).

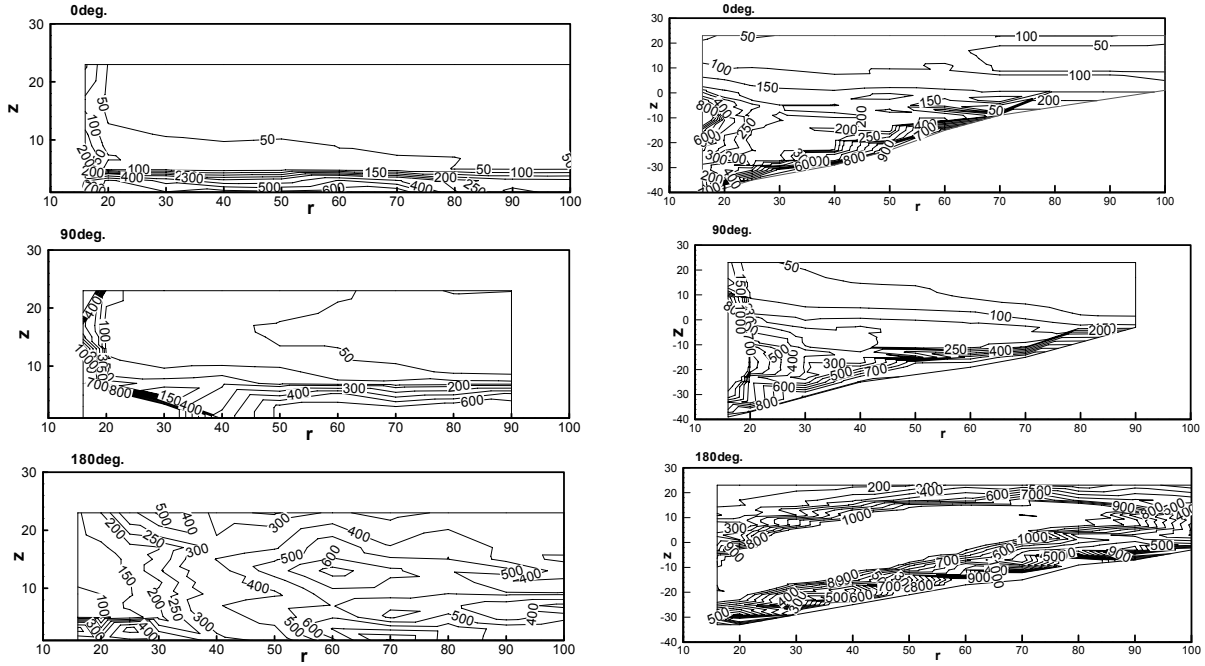

Figure 6. Contours of radial turbulence intensity $\sqrt{v'v'}$ (in cm/s) at azimuthal planes with θ =0, 90 and 180º for plane bed (left) and for scoured bed (right).

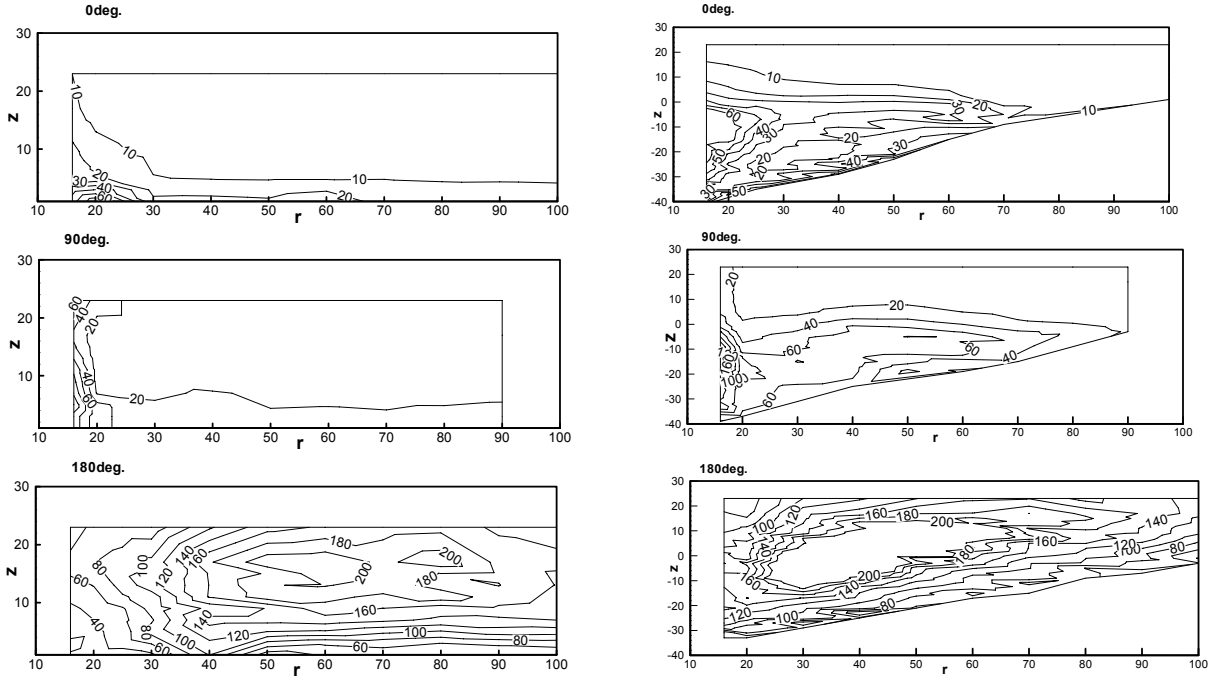

Figure 7. Contours of vertical turbulence intensity $\sqrt{w'w'}$ (in cm/s) at azimuthal planes with θ =0, 90 and 180º for plane bed (left) and for scoured bed (right).

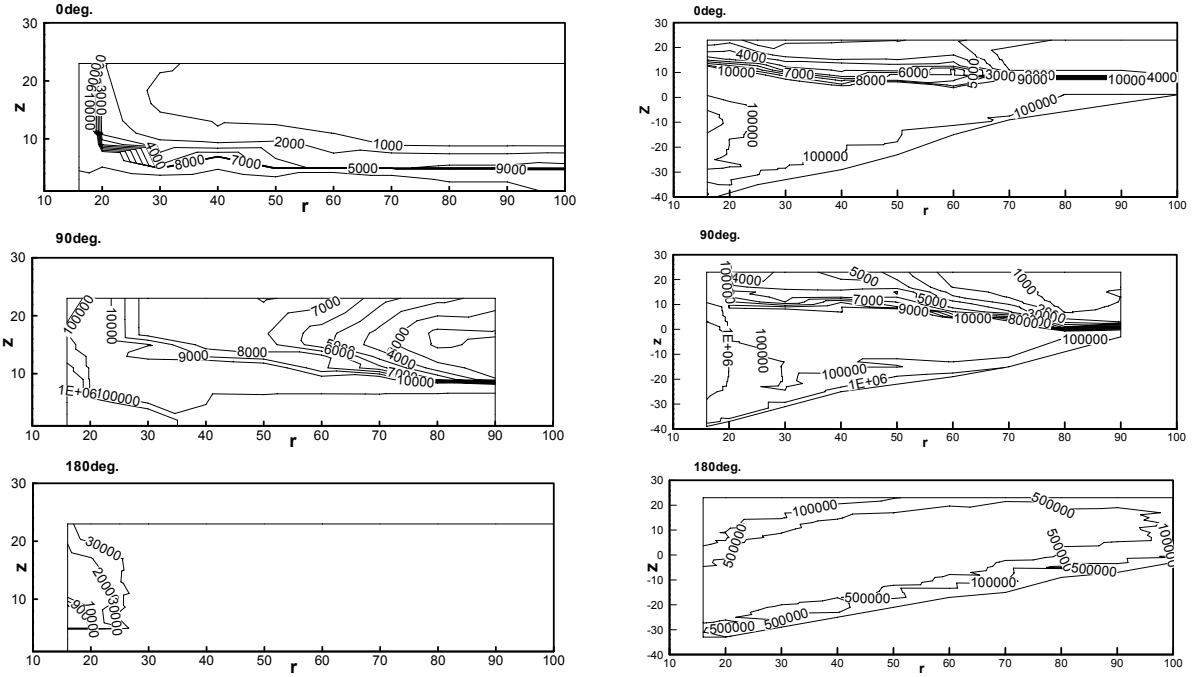

Figure 8. Contours of turbulent kinetic energy ***TKE*** (in cm^2/s^2) at azimuthal planes with θ =0, 90 and 180º for plane bed (left) and for scoured bed (right).

4 CONCLUSIONS

An experimental investigation on the three dimensional turbulent flow field around a square cylinder in a uniform gravel bed under the clear water scour condition was presented. Point measurements allowed the quantitative description of the main flow features around a square cylinder in a plane bed and in an equilibrium scour hole. The spatial distribution of time-absolute velocity, flow vectors, turbulence intensities components and turbulent kinetic energy using acoustic Doppler velocimeter ADV has been presented. The results are useful for validation of CFD models that can be used to simulate scouring around bridge elements improving their design.

ACKNOWLEDGEMENTS

Authors greatly acknowledge the financial support provided by the Egyptian Government through a PhD Grant of the first author, the german research council, DFG for grant ZA 93/14-1, and the Chilean research council CONICYT for grant FONDECYT 11080126.

REFERENCES

Dey, S., 1995. Three-dimensional vortex flow field around a circular cylinder in a quasi-equilibrium scour Hole. Acad. Sci., 20 (December), 871–885.

Dey, S. and Raikar, R., 2007. Characteristics of horseshoe vortex in developing scour holes. Journal of Hydraulic Engineering, 133(4), 399-413.

Diab, R., Link, O. and Zanke, U., 2008. Measuring developing scour holes in gravel. 4th International Conference on Scour and Erosion, ICSE-4. Tokyo, 486-490.

Diab, R., Link, O. and Zanke, U., 2009. Experimental investigation of 3D flow field around square pier. 33rd IAHR Congress, Vancouver, 5460-5466.

Diab, R., Link, O. and Zanke, U., 2010. Geometry of developing and equilibrium scour holes at bridge piers in gravel. Canadian Journal of Civil Engineering, 37(4), 544-554.

Gobert, C., Link, O., Manhart, M. and Zanke, U., 2009. Discussion of coherent structures in the flow field around a circular cylinder with scour hole by G. Kirkil, S. G. Constaninescu and R. Ettema. Journal of Hydraulic Engineering. (in press).

Kirkil, G., Constantinescu, S. and Ettema, R., 2008. Coherent structures in the flow field around a circular cylinder with scour hole. J. of Hydr. Eng., 134(5), 572-587.

Kirkil, G., Constantinescu, G., Ettema, R., 2009. Detached eddy simulation investigation of turbulence at a circular pier with scour hole. J. of Hydr. Eng., 135(11), 888-901.

Link, O., Gobert, Ch., Manhart, M. and Zanke, U., 2008a. Effect of the horseshoe vortex system on the geometry of a developing scour hole at a cylinder". 4th International Conference on Scour and Erosion, Tokyo, 162-168.

Link, O., Pfleger, F. and Zanke, U., 2008b. Characteristics of developing scour-holes at a sand-embedded cylinder. International Journal of Sediment Research, 23(3), 268-276.

Muzzammil, M. and Gangadhariah, T., 2003. The mean characteristics of horseshoe vortex at a cylindrical pier. Journal of Hydraulic Research, 41(3), 285-297.

Raikar, R. and Dey, S., 2005. Clear-water scour at bridge piers in fine and medium gravel beds. Canadian Journal of Civil Engineering, (32), 775-781.

Raikar, R. and Dey, S., 2005. Scour of gravel beds at bridge piers and abutments. Water Management, (158) 157-162.

Unger, J. and Hager, W., 2007. Down-flow and horseshoe vortex characteristics of sediment embedded bridge piers. Exp. Fluids, (42),1-19.

Zanke, U., 1982. Basic of Sediment Motion (Grundlagen der Sedimentbewegung). Springer Verlag, Berlin 1982, P. 353 - 366.